JACS
JOURNAL OF THE AMERICAN CHEMICAL SOCIETY

Subscriber access provided by American Chemical Society

Article

Oxidative Activation of *n*-Butane on Sulfated Zirconia

Xuebing Li, Katsutoshi Nagaoka, Laurent J. Simon, Roberta Olindo, Johannes A. Lercher, Alexander Hofmann, and Joachim Sauer

J. Am. Chem. Soc., **2005**, 127 (46), 16159-16166• DOI: 10.1021/ja054126d • Publication Date (Web): 27 October 2005

Downloaded from http://pubs.acs.org on March 25, 2009

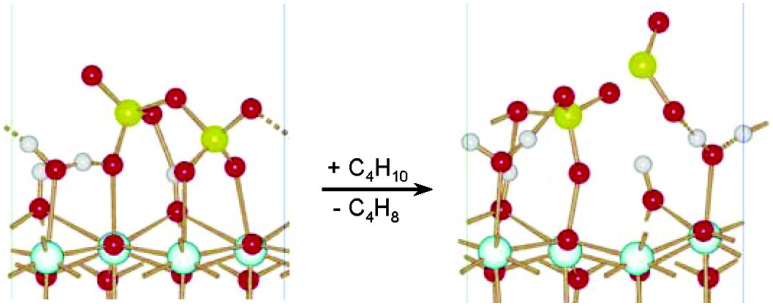

More About This Article

Additional resources and features associated with this article are available within the HTML version:

- Supporting Information
- Links to the 6 articles that cite this article, as of the time of this article download
- Access to high resolution figures
- Links to articles and content related to this article
- Copyright permission to reproduce figures and/or text from this article

View the Full Text HTML

ACS Publications
High quality. High impact.

Journal of the American Chemical Society is published by the American Chemical Society. 1155 Sixteenth Street N.W., Washington, DC 20036

J|A|C|S
ARTICLES
Published on Web 10/27/2005

Oxidative Activation of *n*-Butane on Sulfated Zirconia

Xuebing Li,[†,¶] Katsutoshi Nagaoka,[†,§] Laurent J. Simon,[†,#] Roberta Olindo,[†] Johannes A. Lercher,*[,†] Alexander Hofmann,[‡] and Joachim Sauer*[,‡]

Contribution from the Lehrstuhl für Technische Chemie II, Technische Universität München, Lichtenbergstrasse 4, 85747 Garching, Germany, and Institut für Chemie, Humboldt-Universität zu Berlin, Unter den Linden 6, 10099 Berlin, Germany

Received June 22, 2005; E-mail: johannes.lercher@ch.tum.de; js@chemie.hu-berlin.de

Abstract: Catalytic activation and conversion of light alkanes by sulfated zirconia is unequivocally shown to be initiated by producing small concentrations of olefins. This occurs via stoichiometric oxidative dehydrogenation of butane by SO_3 or pyrosulfate groups to butene (present mostly as alkoxy groups), water, and SO_2. Thermal desorption and in situ IR spectroscopy have been used to determine all three reaction products. The concentration of butene formed determines both the catalytic activity of sulfated zirconia as well as the deactivation via formation of oligomers. The thermodynamics of the oxidative dehydrogenation of *n*-butane by different SZ surface structures has been examined by density functional (DFT) calculations. The calculations show that pyrosulfate or re-adsorbed SO_3 species have the highest oxidizing ability.

1. Introduction

Solid acids are environmentally benign catalysts for low-temperature activation and transformation of alkanes. Among these, sulfated zirconia (SZ) attracted marked interest during the past two decades[1] because of its high catalytic activity for light alkane skeletal isomerization at low temperatures.[2,3]

Most reports suggest that carbenium-type intermediates are the active species during catalysis at steady state. However, the mechanism of the carbenium ion formation is discussed controversially.

Gates et al.[4] suggested that the catalytic activity of modified SZ for the conversion of propane, ethane, and methane is caused by the protolytic activation of short alkanes, such as shown occurring via carbonium ions with superacids in the liquid phase.

Later, however, it has been shown that SZ possesses high acid strength, but its strength does not exceed that of sulfuric acid, HZSM-5, or H-mordenite.[5] This conclusion has also been supported by density functional calculations.[6] Thus, considering the temperatures at which *n*-butane isomerization takes place, the reaction pathway via carbonium ions seems unlikely.

At the same time, Tabora et al.[7] observed that SZ exhibited extremely low catalytic activity for *n*-butane isomerization after removing all butene impurities in the feed. Thus, it was proposed that the butene impurities present in the reactant initiate the *n*-butane reactions on SZ, via formation of carbenium ion intermediates.

However, as SZ still shows catalytic activity for *n*-butane isomerization after removal of butene impurities, it has been suggested that butene species are formed in situ. Fărcaşiu et al.[8] ascribed the initial activity to carbocation precursors formed through one electron oxidation of the alkane by sulfate groups. The promoting effect of transition metal doping SZ was also attributed to the enhancement of the oxidative properties.[9] While direct evidence for the surface reduction step involved in the activation of butane has not been given, indirect kinetic evidence for olefin formation has been reported.[10] The formation of butene by the oxidative species of SZ or promoted SZ could follow eq 1.

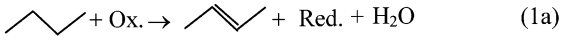

(1a)

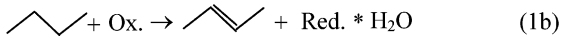

(1b)

In the gas phase, with the oxidizing species being SO_3 and the reduced species being SO_2, this is an exothermic process

[†] Technische Universität München.
[‡] Humboldt-Universität zu Berlin.
[¶] Present address: Department of Chemical Engineering, University of California at Berkeley, Berkeley, CA 94720 USA.
[§] Present address: Department of Applied Chemistry, Faculty of Engineering, Oita University, Dannoharu 700, Oita 870-1192, Japan.
[#] Present address: IFP-Lyon, Catalysis and Separation Department, BP-3, 69390 Vernaison, France.

(1) Song, X.; Sayari, A. *Catal. Rev.—Sci. Eng.* **1996**, *38*, 329−412.
(2) (a) Holm, V. C. F.; Bailey, G. C. US Patent 3,032,599, 1962. (b) Hino, M.; Kobayashi, S.; Arata, K. *J. Am. Chem. Soc.* **1979**, *101*, 6439−6441. (c) Hino, M.; Arata, K. *J. Chem. Soc., Chem. Commun.* **1980**, *18*, 851−852.
(3) (a) Adeeva, V.; Liu, H.; Xu, B.; Sachtler, W. M. H. *Top. Catal.* **1998**, *6*, 61−76. (b) Ono, Y. *Catal. Today* **2003**, *81*, 3−16. (c) Sommer, J.; Jost, R.; Hachoumy, M. *Catal. Today* **1997**, *38*, 309−319.
(4) (a) Cheung, T. K.; Gates, B. C. *J. Chem. Soc., Chem. Commun.* **1996**, *16*, 1937−1938. (b) Cheung, T. K.; Gates, B. C. *J. Catal.* **1997**, *168*, 522−531. (c) Cheung, T. K.; Lange, F. C.; Gates, B. C. *J. Catal.* **1996**, *159*, 99−106. (d) Rezgui, S.; Liang, A.; Cheung, T. K.; Gates, B. C. *Catal. Lett.* **1998**, *53*, 1−2.
(5) (a) Umansky, B. S.; Hall, W. K. *J. Catal.* **1990**, *124*, 97−108. (b) Babou, F.; Coudurier, G.; Védrine, J. C. *J. Catal.* **1995**, *152*, 341−349.
(6) Haase, F.; Sauer, J. *J. Am. Chem. Soc.* **1998**, *120*, 13503−13512.
(7) Tábora, J. E.; Davis, R. J. *J. Am. Chem. Soc.* **1996**, *118*, 12240−12241.
(8) (a) Srinivasan, R.; Keogh, R. A.; Ghenciu, A.; Fărcaşiu, D.; Davis, B. H. *J. Catal.* **1996**, *158*, 502−510. (b) Fărcaşiu, D.; Ghenciu, A.; Li, J. Q. *J. Catal.* **1996**, *158*, 116−127.

with a reaction enthalpy of −28 kJ/mol.[11] DFT calculations reported below show that on the surface of SZ (eq 1b) the corresponding reaction might be even more exothermic, with reaction energies up to −67 kJ/mol. In a previous paper, we have shown that the surface species is not just supported H_2SO_4, but that the presence of re-adsorbed SO_3 generated from labile sulfate groups is critical for an active catalyst.[12] Removing the labile fraction of the sulfate groups led to the complete disappearance of the catalytic activity.

In this work, unequivocal direct evidence for all three potential reaction products of the initial alkane oxidation is given using thermal desorption/reaction of *n*-butane, in situ (operando) IR spectroscopy, and quantification of the SO_2 formed on the catalyst. It is emphasized that *n*-butane used in this study was carefully purified from traces of olefin. To demonstrate the subtle influences of the reaction conditions, the catalytic results are also compared with the conversion of unpurified *n*-butane and with the conversion of the purified *n*-butane in the presence of hydrogen or oxygen. DFT calculations with periodic boundary conditions are carried out to explore the thermodynamics of the reduction of different SZ surface structures by *n*-butane and the accompanying water adsorption.

Previously, DFT calculations have been made on the (non-oxidative) dehydrogenation of isobutane yielding isobutene using a minimal size model of SZ.[13] The reaction energy reported (+155 kJ/mol) indicates that this process is thermodynamically much less favorable than the oxidative dehydrogenation considered in this study.

2. Experimental Section

2.1. Catalytic Material and Conditioning. Sulfate-doped zirconium hydroxide was obtained from Magnesium Electron, Inc. (XZO 1077/01). The as-received sample was heated to 873 K with an increment of 10 K/min for 3 h in static air with a bed depth of 3 cm to form SZ with 0.44 mmol sulfate/g and a specific surface area of 109 m^2/g.

2.2. Catalyst Characterization. The ***temperature-programmed desorption and reaction (TPD)*** of *n*-butane from SZ was conducted in vacuum. The SZ sample (0.1 g) was activated in vacuum ($p = 10^{-3}$ mbar; vacuum cell volume approximately 20 mL) at 673 K for 2 h and cooled to 323 K for *n*-butane adsorption; 2 mbar of *n*-butane (purified with an olefin trap containing activated commercial zeolite HY; residual olefin content below the detection limit of 1 ppm) was allowed to equilibrate with the sample for 5 min. After reducing the pressure to 10^{-3} mbar, TPD was carried out up to 873 K with a heating increment of 10 K/min. The desorbing species were detected by a mass spectrometer (QME 200, Pfeiffer vacuum).

To ***determine the amount of SO_2 produced***, 100 mL of 0.005 N NaOH solution in a washing flask was used to collect SO_2 and SO_3 in the educts during activation, *n*-butane reaction and temperature-programmed desorption after the reaction. The gases were trapped as sulfate and sulfite. Only the sulfate concentrations were determined by ion chromatography (Metrohm, 690 ion chromatograph equipped with an IC anion column). Sulfite was oxidized in a second experiment with H_2O_2 (200 μL, 30%), and the solution was re-analyzed. The concentration of sulfite was determined from the difference between the two experimental results.

In situ IR spectroscopy was used to monitor adsorbed species during *n*-butane isomerization using a Bruker IFS 88 spectrometer at 4 cm^{-1} resolution. A self-supporting wafer (5−10 mg/cm^2) was prepared by compacting the sample. The wafer was placed into in a stainless steel cell with CaF_2 windows, heated at a rate of 10 K/min to 673 K in He flow (10 mL/min), and activated at that temperature for 2 h. The wafer was then cooled to 373 K, and the reactant mixture (5% *n*-butane in He, total flow of 20 mL/min) was flown into the cell. A spectrum was collected every minute. *n*-Butane was purified with an olefin trap containing activated HY zeolite to remove the butene impurities.

2.3. Catalytic Conversion of *n*-Butane. *n*-Butane (99.5%) isomerization was carried out in a quartz microtube reactor (8 mm inner diameter) under atmospheric pressure; 0.2 g of SZ pellets (355−710 μm) was loaded into the reactor and activated in situ at 673 K for 2 h in He flow (10 mL/min). The catalyst was cooled to 373 K, and the reactant mixture (5% *n*-butane in He, total flow of 20 mL/min) was flown through the catalyst bed. *n*-Butane was passed through the olefin trap containing activated HY zeolite, before it was mixed with He. The butene concentration in the resulting gas was below the detection limit (1 ppm). Reaction products were analyzed on-line using an HP 5890 gas chromatographer (GC) equipped with a capillary column (Plot Al_2O_3, 50 m × 0.32 mm × 0.52 μm) connected to a flame ionization detector (FID).

The skeletal isomerization of unpurified *n*-butane, containing 26 ppm 2-butene (molar basis), on SZ at 373 K was also performed to investigate the influence of butene impurities in the feed.

n-Butane isomerization at 373 K was carried out also in the presence of different concentrations of hydrogen or oxygen for studying the influence of enhancing or reducing the concentration of olefins on the catalytic activity.

2.4. Computational Methods. The density functional calculations use the gradient-corrected Perdew−Wang functional, PW91.[14] Core electrons are described with the projector augmented wave scheme.[15] The valence electrons are described by a plane wave basis set with an energy cutoff of 400 eV. Periodic boundary conditions are applied to an 1 × 2 surface cell of the *t*-ZrO_2(101), which includes four zirconium atoms, which miss one coordination compared to the bulk. A slab of five layers is used with three bottom layers fixed to the bulk positions. The cell size is $a = 6.425$ Å, $b = 7.284$ Å, and $c = 30.000$ Å. Further details are given in ref 16. All calculations are made with the VASP code.[17]

3. Results

3.1. Determination of the Reaction Products of the Initiation Reaction. The initiation reaction as formulated in eq 1 is a stoichiometric (in contrast to catalyzed) reaction to produce butene, SO_2, and H_2O. The overall catalytic reaction requires, however, that the majority of catalytic cycles occurs in a way that does not require oxidation for the formation of the carbenium ions, that is, that an efficient mechanism of chain propagation (hydrogen transfer) exists. The experiments below establish that all three reaction products exist and that water and SO_2 do not leave the surface, while the majority of butene molecules is in adsorption−desorption equilibrium.

(9) (a) Adeeva, V.; de Haan, J. W.; Jänchen, J.; Lei, G. D.; Schünemann, V.; van de Ven, L. J. M.; Sachtler, W. M. H.; van Santen, R. A. *J. Catal.* **1995**, *151*, 364−372. (b) Wan, K. T.; Khouw, C. B.; Davis, M. E. *J. Catal.* **1996**, *158*, 311−326.
(10) Liu, H.; Adeeva, V.; Lei, G. D.; Sachtler, W. M. H. *J. Mol. Catal A: Chem.* **1995**, *100*, 35−48.
(11) http://webbook.nist.gov.
(12) Li, X.; Nagaoka, K.; Lercher, J. A. *J. Catal.* **2004**, *247*, 130−137.
(13) Hong, Z.; Fogash, K. B.; Watwe, R. M.; Kim, B.; Masqueda-Jimenez, B. I.; Natal-Santiago, M. A.; Hill, J. M.; Dumesic, J. A. *J. Catal.* **1998**, *178*, 489−498.
(14) (a) Perdew, J. P. *Phys. Rev. B* **1986**, *33*, 8822−8824. (b) Perdew, J. P. *Phys. Rev. B* (*Errata*) **1986**, *34*, 7406. (c) Perdew, J. P. In *Electronic Structure of Solids;* Ziesche, P., Eschrig, H., Eds.; Akademie Verlag GmbH: Berlin, 1991.
(15) (a) Blöchl, P. E. *Phys. Rev. B* **1994**, *50*, 17953−17979. (b) Kresse, G.; Joubert, J. *Phys. Rev. B* **1999**, *59*, 1758−1775.
(16) Hofmann, A.; Sauer, J. *J. Phys. Chem. B* **2004**, *108*, 14652−14662.
(17) (a) Kresse, G.; Furthmüller, J.; Hafner, J. *Europhys. Lett.* **1995**, *32*, 729−734. (b) Kresse, G.; Furthmüller, J. *Comput. Mater. Sci.* **1996**, *6*, 15−50. (c) Kresse, G.; Furthmüller, J. *Phys. Rev. B* **1996**, *54*, 11169−11186.

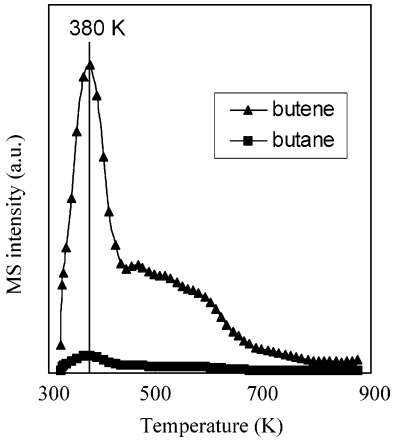

Figure 1. Desorption peaks of butene (▲ $m/e = 56$) and butane (■ $m/e = 58$) during TPD after adsorption at 323 K of 2 mbar of *n*-butane on activated sulfated zirconia.

3.1.1. Evidence for Butene Formation by TPD of *n*-Butane. Under steady state conditions at 373 K, butenes are not detected in the reaction products. Thus, temperature-programmed reaction/desorption of adsorbed *n*-butane has been used to explore whether butene is formed in the initiating step. Figure 1 shows the evolution of butane and butene from SZ during TPD after *n*-butane adsorption at 323 K.

Butene ($m/e = 56$) desorbed at low temperatures with a maximum rate at 380 K and a broad shoulder between 500 and 700 K. Note that much lower rates and quantities of desorbing *n*-butane were observed, as most of it was already removed by the short evacuation period prior to TPD. Fragments larger than butane were not observed. However, some CO_2 desorbed at 580 K. The fragmentation pattern observed in the mass spectra agrees perfectly with the fragmentation pattern of butenes, allowing one to exclude the presence of other alkanes or alkenes. Thus, TPD of *n*-butane shows that a mixture of linear butenes is formed from butane adsorbed on SZ at low temperatures. The maximum temperature of the evolution demonstrates that butene is easily desorbed from the surface at typical reaction temperatures (273−373 K), so that it is fully equilibrated with the gas phase.

Molecular hydrogen was not observed during these experiments, allowing one to exclude a route via the direct dehydrogenation. While we cannot confirm the continuous production of H_2 reported previously,[13] we would like to point out that the labile SO_3 species on the surface would convert any hydrogen formed to water and SO_2.

However, water and SO_2, the expected products of the oxidation reaction, were also not detected in parallel to the desorbing butene. In contrast to H_2, which is only very weakly adsorbed on the sulfate-modified oxides, water and SO_2 are expected to be so strongly adsorbed that desorption might be delayed to higher temperatures and so being partly masked by the potential partial decomposition and dehydration of SZ. It should also be noted that the mass spectrometric analysis is ambiguous in differentiating between desorbing SO_2 and SO_3.

3.1.2. Determination of SO_2 Formed. To qualitatively and quantitatively determine desorbing SO_x, the gases exiting the reactor were passed through a washing solution containing NaOH. For this purpose, a larger catalyst bed (2 g of SZ) was used. With this method, desorbed SO_3 leads directly to sulfates, while SO_2 leads to sulfites that have to be oxidized by H_2O_2 to be detected. Each solution was, therefore, also treated with H_2O_2 to differentiate between the formation of SO_2 and SO_3.

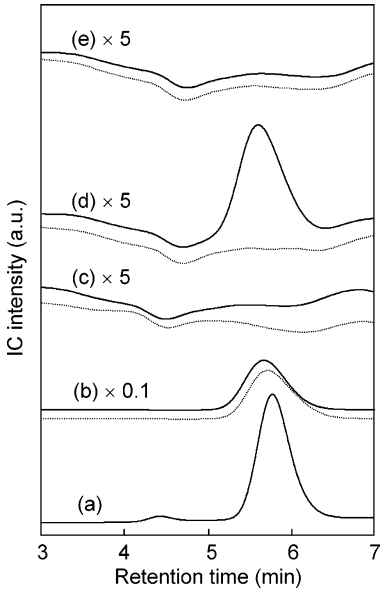

Figure 2. Sulfate ion peaks in IC spectra recorded without adding H_2O_2 (· · ·) and adding H_2O_2 (—): (a) 5 mg/L of sulfate as standard, (b) after activation of sulfated zirconia at 673 K in He, (c) after reaction at 373 K for 10 h, (d) after increasing temperature from 373 to 673 K following reaction for 10 h, and (e) after increasing temperature from 373 to 673 K following the He treatment at 373 K.

The sulfate ion peaks in the ion chromatography trace are shown in Figure 2.

During activation up to 673 K, a small amount of sulfate species decomposed and desorbed as SO_3 from the catalyst (see Figure 2b; the solid line refers to the total SO_2 and SO_3 content, not corrected for SO_3 detected before oxidation by H_2O_2). This amount corresponded to 3% of the total sulfate content of the SZ studied. During 10 h reaction at 373 K, sulfur compounds did not evolve from the reactor (see Figure 2c). Thus, we concluded that SO_2 was either not formed during reaction or, if it was, it was retained on the catalyst surface as a sulfite group.

To differentiate between the two possibilities, the reactor was purged with He for 30 min. Then, the temperature was increased with 10 K/min to 673 K in He flow. In contrast to the activation of SZ, the solution of the trapped gases showed only a significant amount of sulfate ions after oxidation with H_2O_2 (Figure 2d). Thus, we conclude that SO_2 and not SO_3 evolved from the catalyst. Approximately 0.2% of the total sulfate species in SZ was detected to be reduced by reaction with *n*-butane for 10 h. The control experiment of increasing the temperature from 373 to 673 K after exposing the activated catalyst to flowing He at 373 K did not lead to the evolution of SO_x (Figure 2e). Note that the lack of detection of SO_2 from sulfated zirconia (after reaction with benzene) upon heating below 673 K, as reported in ref 8a, is due to the drastically lower sensitivity used in those experiments unable to identify 0.2% of the total sulfur content released as SO_2.

3.1.3. Determination of Water Formed by In Situ IR Spectroscopy. Having shown that butene and SO_2 are formed in the initiation step, the formation of water was followed by in situ IR spectroscopy under reaction conditions. The in situ IR spectra of SZ during *n*-butane conversion at 373 K are shown

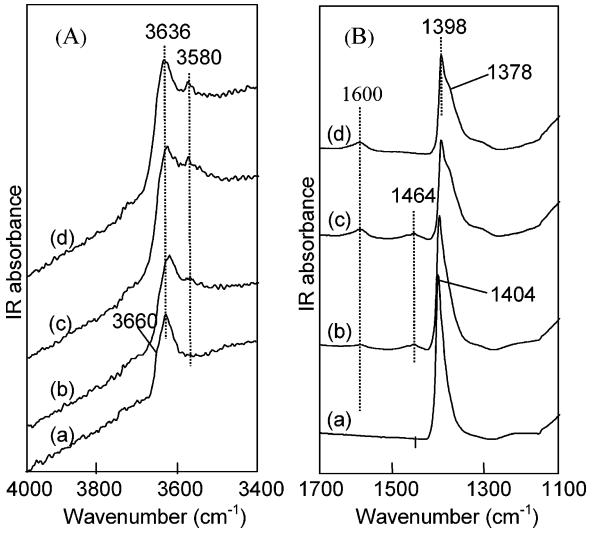

Figure 3. In situ IR spectra of sulfated zirconia recorded (a) after activation, (b) after 60 min isomerization reaction (373 K, 20 mL/min 5% *n*-butane in He), (c) after 180 min isomerization reaction, and (d) after 10 min He purge following the reaction.

in Figure 3A and B. After activation at 673 K for 2 h, the SZ sample showed a strong band at 3636 cm^{-1} with a shoulder at 3660 cm^{-1} and a weak band at 3580 cm^{-1} in the region of OH groups. The bands at 3636 and 3580 cm^{-1} are attributed to OH groups associated with the sulfate groups, while the shoulder at 3660 cm^{-1} is associated with ZrOH groups.[18,19] In contact with butane, a weak broad band between 3500 and 3600 cm^{-1} appeared, which is attributed to butane hydrogen bonding to OH groups by polarizing the alkane C−H bond.[20] Additionally, the IR band at 3580 cm^{-1} increased in intensity.

The sulfate stretching bands of activated SZ appeared at 1300−1450 cm^{-1} with a maximum at 1404 cm^{-1}, which is assigned to the stretching vibrations of the S═O bond (see Figure 3B) in pyrosulfate groups or adsorbed SO_3 molecules. This assignment is based on previous DFT calculations.[16] During *n*-butane isomerization, this band broadened and shifted to lower wavenumbers, that is, to 1398 cm^{-1} with a shoulder at 1378 cm^{-1} after reaction for 200 min and persisting after evacuation. The band at 1464 cm^{-1} observed after bringing SZ in contact with butane is assigned to the CH_2 deformation vibration of butane. It disappeared after He purge for 10 min.

The formation of water during reaction is shown by the increasing intensity of the water deformation band at 1600 cm^{-1} with the time on stream. The band has been identified to be caused by the water deformation vibration through exposing SZ to H_2O. As shown in Figure 4, the evolution of the catalytic activity in the induction period occurred in parallel to concentration of water formation. The gradual formation of water on SZ indicates that the oxidation of *n*-butane at 373 K is the determining step for building up of active species, which corresponds to the period of increasing activity in *n*-butane isomerization.

Once the steady state of the isomerization reaction had been reached, the rate of accumulation of water was significantly

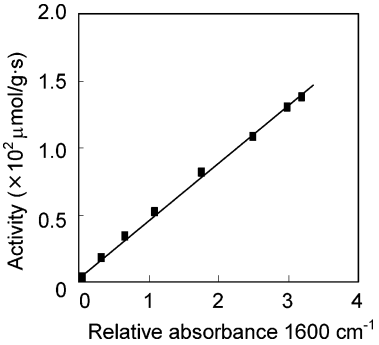

Figure 4. Correlation between catalytic activity of sulfated zirconia for *n*-butane isomerization at 373 K during induction period and the concentration of water formed during in situ IR reaction.

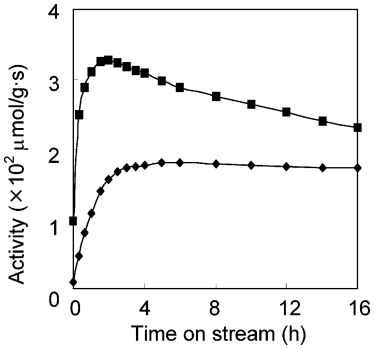

Figure 5. Catalytic activity of sulfated zirconia at 373 K for the isomerization reaction of *n*-butane (20 mL/min 5% *n*-butane in He) (◆) purified with olefin trap, and (■) unpurified and containing 26 ppm 2-butene.

slower. This slower rate is attributed to the strong perturbation of the sulfate/SO_3 groups by water formed, shifting the band from 1404 to 1398 cm^{-1} and reducing the oxidation ability of sulfate groups/adsorbed SO_3. The fact that the formation of water did not cease at steady state shows, however, that part of the labile sulfate/SO_3 groups react further and produce butene, to replace those carbenium ions that have been lost by desorption or oligomerization with other butene molecules.

3.2. Promoting Effect of Butene Impurities on the Catalytic Activity. Figure 5 shows the *n*-butane isomerization activity versus time on steam (TOS) on SZ at 373 K with purified and unpurified *n*-butane. The butene impurities significantly enhanced the catalytic activity, in agreement with ref 7. Both experiments showed a period of increasing activity, during which the active species, that is, carbenium-type intermediates, SO_2, and water, accumulate on the surface. Reaching the maximum activity was followed by gradual deactivation. The induction period for the reaction of purified *n*-butane was around 4 h, which was much longer than that of reactant without purification (1.5 h) under identical reaction conditions. The isobutane selectivity in both experiments was higher than 95%, and the byproducts of the reaction were primarily propane, isopentane, and *n*-pentane (the ratio of iso- to *n*-pentane was 4−5). Thus, the presence of butene influences the activity and deactivation, but not the selectivity of the reaction.

3.3. Influence of H_2 and O_2 on the Catalytic Activity. On the basis of the important role of butene formation via the oxidative route, hydrogen and oxygen can be assumed to lead to two important consequences for the overall reaction.

(18) Bensitel, M.; Saur, O.; Lavalley, J. C.; Mabilon, G. *Mater. Chem. Phys.* **1987**, *17*, 249−258.
(19) Morterra, C.; Cerrato, G.; Pinna, F.; Strukul, G. *Catal. Lett.* **2001**, *73*, 113−119.
(20) Eder, F.; Stockenhuber M.; Lercher, J. A. *J. Phys. Chem. B* **1997**, *101*, 5414−5419.

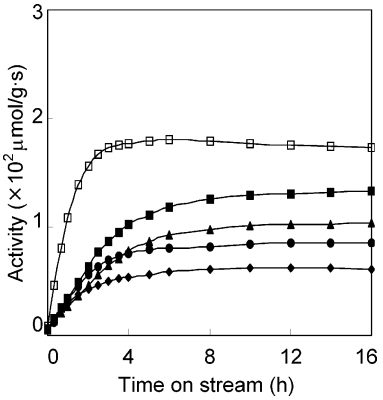

Figure 6. Catalytic activity of sulfated zirconia for the isomerization reaction of *n*-butane (20 mL/min 5% *n*-butane in He) at 373 K in the presence of different concentrations of hydrogen in the feed: (□) 0%, (■) 0.5%, (▲) 1.5%, (●) 2.5%, (◆) 5%.

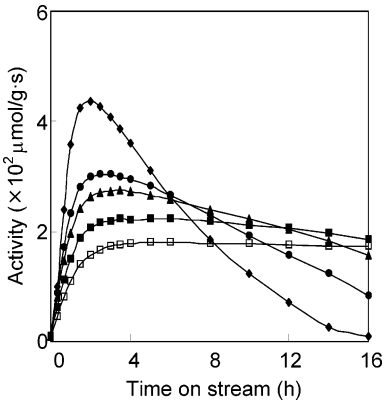

Figure 7. Catalytic activity of sulfated zirconia for the isomerization reaction of *n*-butane (20 mL/min 5% *n*-butane in He) at 373 K in the presence of different concentrations of oxygen in the feed: (□) 0%, (■) 0.5%, (▲) 1.5%, (●) 2.5%, (◆) 5%.

H_2 has been observed with zeolite-based catalysts to effectively suppress hydride transfer by acting as hydride donor, forming an alkane and restoring the acid site. Thus, in the presence of hydrogen, the rate should be reduced by requiring a larger fraction of oxidation cycles and a lower overall concentration of olefins and/or carbenium ions. The reaction rates versus time on stream in the presence of different hydrogen concentrations are shown in Figure 6. The presence of hydrogen in the feed, even at 0.5% concentration, significantly lowered the catalytic activity, in agreement with previous observations.[21]

Figure 7 shows the influence of the presence of oxygen on the catalytic activity. With increasing oxygen partial pressure, the initial increase in activity was higher and the subsequent deactivation with TOS was more rapid. For instance, the catalyst operated in the presence of 5% oxygen was completely deactivated after 16 h TOS, while the one in the absence of oxygen or in the presence of hydrogen still had a very stable activity. The high activity is explained by the formation of very reactive sulfate groups and the reoxidization of sulfite groups. This leads to an enhanced production of olefins, which not only produce more carbenium-type intermediates but also alkylate the existing carbenium ions, leading to larger fragments on the surface.

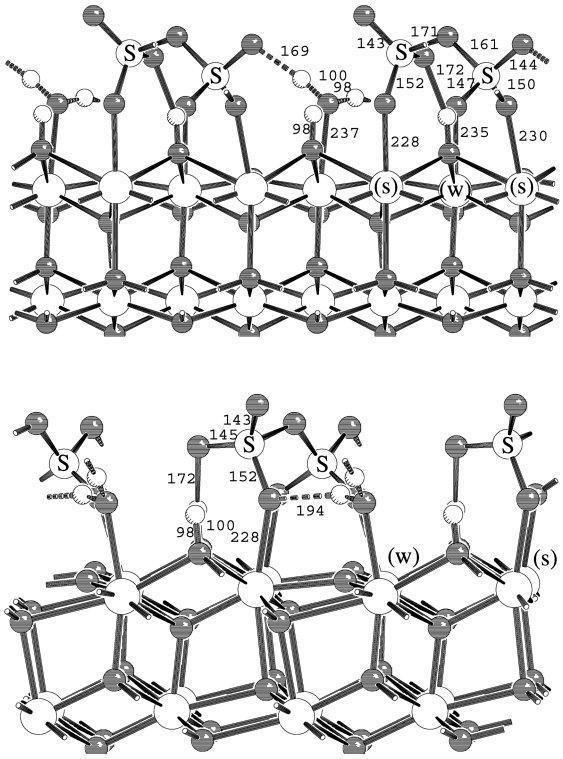

Figure 8. Structure of $[S_2O_7^{2-},2H^+,H_2O]$.

3.4. Calculated Reduction Energies and Vibrational Frequencies for Different Surface Structures. In a previous DFT study, we have calculated the structures and stabilities of different surface species for increasing loading of H_2SO_4 or SO_3 and H_2O adsorbed on the (101) surface of *t*-ZrO_2.[16] For a given composition, different "isomeric" surface structures are examined and their stabilities compared. For example, H_2O can dissociate on the surface into H^+ and OH^- and form a bridging and a terminal hydroxyl group. The surface composition is written in brackets, for example, $[SO_3,OH^-,H^+,H_2O]$ denotes a surface phase with one SO_3 and two H_2O molecules adsorbed on a 1 × 2 *t*-ZrO_2(101) surface cell. One water molecule is dissociatively adsorbed. The surface phase $[SO_4^{2-},OH^-,3H^+]$ has the same total composition, one SO_3 and two H_2O molecules on the surface, but $SO_3{\cdot}H_2O$ is present as H_2SO_4, which is dissociatively adsorbed as SO_4^{2-}, $2H^+$, and the second H_2O molecule is also dissociatively adsorbed.

The relative stability of surface structures with different compositions depends on the concentration of sulfur-containing species in the gas phase with which the surface is assumed to be in equilibrium. If we assume equilibrium with H_2SO_4/H_2O and SO_3/H_2O, the pyrosulfate phase $[S_2O_7^{2-},2H^+,H_2O]$ (Figure 8) and the proton-free $[SO_3]$ phase, respectively, are the prevailing surface structures for wide temperature and partial pressure ranges. The vibrational spectra discussed in section 3.1.3. (Figure 3B) point to the presence of pyrosulfate species in the SZ sample used. Only for loadings of two sulfate groups per 1 × 2 *t*-ZrO_2(101) surface cell S═O vibrations above 1400 cm^{-1} are predicted, and only pyrosulfate species have S═O vibrations in the region of 1420−1400 cm^{-1}.[16] (Note that this assignment contradicts earlier suggestions[22] that a S═O Raman

(21) Garin, F.; Andriamasinoro, D.; Abdulsamad, A.; Sommer, J. *J. Catal.* **1991**, *131*, 199−203.

(22) Riemer, T.; Spielbauer, D.; Hunger, M.; Merkhener, G. A. H.; Knözinger, H. *J. Chem. Soc., Chem. Commun.* **1994**, *10*, 1181−1182.

Table 1. Reduction Energy, ΔE_{red}, for the Loss of $^1/_2$ O_2 of Different SZ Structures (in kJ/mol)

	ΔE_{red}	ΔH_{red}^{298K}	ΔH_{red}^{398K}
pure 1 × 2 *t*-ZrO_2(101)	554.5		
$[SO_3]^a$	173.2	174.1	166.2
$[SO_3,OH^-,H^+]$	177.6		
$[SO_4^{2-},2H^+]$	179.2		
$[SO_3,OH^-,H^+,H_2O]^a$	199.9	199.4	191.6
$[SO_4^{2-},2H^+,OH^-,H^+]$	189.9		
$[SO_4^{2-},2H^+,3H_2O]^a$	184.8	184.5	176.0
$[2SO_3]^a$	161.8	163.0	155.1
$[S_2O_7^{2-},2H^+]$	106.3	109.5	101.6
$[S_2O_7^{2-},2H^+,H_2O]^a$	155.5	156.5	148.4
$[SO_4^{2-},HSO_4^-,3H^+]^a$	164.6	166.4	158.6
$[S_2O_7^{2-},2H^+,2H_2O]$	124.3		
H_2SO_4(gas)	176.3	154.0[b]	153.8
SO_3(gas)	94.3	80.8[c]	80.9

[a] These structures are most stable for specific pressure and temperature regions. [b] Observed value[10] = 196.5 kJ/mol. [c] Observed value[10] = 98.9 kJ/mol.

band at 1399 cm^{-1} is indicative of a triply coordinated O═S(O^-)$_2$(HO^-) structure with C_s symmetry.) Coadsorption of water onto the prevailing $[S_2O_7^{2-},2H^+,H_2O]$ species ($\nu_{S=O}$ = 1421 cm^{-1}), yielding $[S_2O_7^{2-},2H^+,2H_2O]$ ($\nu_{S=O}$ = 1409 cm^{-1}), shifts the S═O band 12 cm^{-1} to lower wavenumbers, as observed during water formation (section 3.1.3.).

To characterize the oxidizing power of SZ, we calculate the reduction energy, ΔE_{red}, that is, the energy of the following reaction:

$$1 \times 2\ t\text{-}ZrO_2(101)\cdot nSO_3\cdot mH_2O \rightarrow 1 \times 2\ t\text{-}ZrO_2(101)\cdot(n-1)SO_3\cdot SO_2\cdot mH_2O + {}^1/_2\ O_2 \quad (2)$$

Table 1 shows the results for the dominating $[SO_3]$ and $[S_2O_7^{2-},2H^+,H_2O]$ phases as well as for phases with a different number of H_2O molecules on the surface. The sulfated surfaces are much more easily reduced than the clean ZrO_2 surface. The reduction energies for the sulfated phases are roughly in the range between the gas phase reduction energies of H_2SO_4 (176 kJ/mol) and SO_3 (94 kJ/mol). They depend on the sulfur concentration of the surface. Surface structures with one SO_3 on the 1 × 2 surface cell have larger reduction energies, between 200 and 173 kJ/mol depending on the number of H_2O molecules on the surface. Surface structures with two SO_3 molecules on the 1 × 2 surface cell have lower reduction energies, between 165 and 106 kJ/mol. The prevailing $[SO_3]$ and $[S_2O_7^{2-},2H^+,H_2O]$ structures have reduction energies of +173 and +156 kJ/mol, respectively. The lowest reduction energy is found for the $[S_2O_7^{2-},2H^+]$ surface structure, +106 kJ/mol.

Table 1 shows also the heats of reduction at 298 and 398 K that differ from the energies by no more than 10 kJ/mol. For the gas phase species, comparison can be made with experimental reaction heats. This indicates an error of about 20 kJ/mol of the calculated values.

4. Discussion

The presented data show for the first time that in the initiation step butene is formed together with water and SO_2. The oxidizing sites are related to re-adsorbed SO_3 (resulting from decomposition of labile sulfate groups) or pyrosulfate groups. Most likely, these are the labile sulfate groups (re-adsorbed SO_3) identified to be indispensable for catalysis in an earlier contribution.[12] The alkene formed is in equilibrium with Brønsted acid sites of SZ by formation of an alkoxy group or carbenium ion, which is the key intermediate. The accumulation of the alkoxy groups/carbenium ions is concluded to be the most important change on the surface during the activation (induction) period. Water and SO_2 also formed in this step remain bound to the surface and reduce the oxidation activity to a much lower level. It should be emphasized that these active sites do not resemble supported H_2SO_4 as it has been proposed in earlier studies.[23]

Table 2. Calculated Total Reaction Energy, ΔE_{total} in (kJ/mol), of Different SZ Structures with *n*-Butane Following C_4H_{10} + 1 × 2 *t*-ZrO_2(101)·nSO_3·mH_2O → C_4H_8 + 1 × 2 *t*-ZrO_2(101)·$(n-1)SO_3$·SO_2·$(m+1)H_2O$

SZ	SZ_{red},OH_2	ΔE_{total}
$[SO_3]^a$	$[SO_2,OH^-,H^+]$	37.1
$[SO_3,OH^-,H^+]$	$[SO_2,OH^-,H^+,H_2O]$	47.0
$[SO_4^{2-},2H^+]$	$[SO_3^{2-},2H^+,OH^-,H^+]$	5.6
$[2SO_3]^a$	$[SO_4^{2-}, SO_2,2H^+]$	−36.1
$[S_2O_7^{2-},2H^+]$	$[S_2O_6^{2-},2H^+,H_2O]$	−66.8
$[S_2O_7^{2-},2H^+,H_2O]^a$	$[SO_4^{2-}, SO_2,2H^+,2H_2O]$	−10.1
$[SO_4^{2-},HSO_4^-,3H^+]^a$	$[S_2O_6^{2-},2H^+,2H_2O]$	−26.7
H_2SO_4 (gas)	$SO_2 + 2H_2O$	68.2
SO_3 (gas)	$SO_2 + H_2O$	−13.8

[a] These structures are most stable for specific pressure and temperature regions.

The favorable reaction energies for the oxidative dehydrogenation of butane according to eq 1 explain the initial butene formation:

$$C_4H_{10} + 1 \times 2\ t\text{-}ZrO_2(101)\cdot nSO_3\cdot mH_2O \rightarrow C_4H_8 + 1 \times 2\ t\text{-}ZrO_2(101)\cdot(n-1)SO_3\cdot SO_2\cdot(m+1)H_2O \quad (3)$$

Table 2 shows the calculated energies for this reaction.

For surface structures with a single sulfur atom per (1 × 2) surface unit cell, the reaction energies are positive (6 to 47 kJ/mol depending on the water content), while structures with two sulfur atoms per cell have negative reaction energies (−10 to −67 kJ/mol). The reaction of one of the dominating pyrosulfate surface structures, $[S_2O_7^{2-},2H^+,H_2O]$, with butane yields the $[SO_4^{2-},SO_2,2H^+,2H_2O]$ structure shown in Figure 9 (reaction energy = −10 kJ/mol). In this reaction, the pyrosulfate splits into a tridentate sulfate species and SO_2, which is not directly coordinated to the surface, but only to two water molecules via two hydrogen bonds (Figure 9). The energy expense for the removal of SO_2 is E_{diss,SO_2} = 34 kJ/mol. The less stable pyrosulfite structure would look like Figure 8, with one oxygen atom removed. Reaction 3 does not consider adsorption of butane/butene on the SZ surface.

In the gas phase, the oxidative dehydrogenation of butane by SO_3 (eq 1a) is also thermodynamically favored. The calculated reaction enthalpy at 298 K is −11 kJ/mol (reaction energy = −14 kJ/mol), and the corresponding experimental value is −28 kJ/mol.[11] The difference of 17 kJ/mol is in the expected error range of DFT calculations.

It should be emphasized that this oxidation chemistry does not occur with supported sulfuric acid on ZrO_2 as it had been discussed and proposed in the literature.[23] While sulfuric acid can be a precursor to the active material, the generation of the labile sulfate/SO_3 species by a high temperature process (calcination) is indispensable for achieving appreciable catalytic activity.

(23) Babou, F.; Coudurier, G.; Védrine, J. C. *J. Catal.* **1995**, *152*, 341−349.

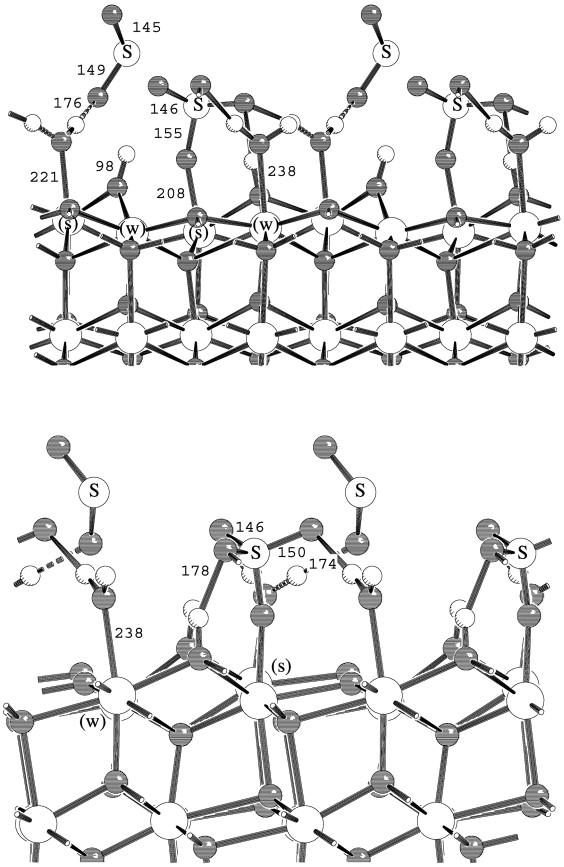

Figure 9. Structure of the reduced $[S_2O_7^{2-},2H^+,H_2O]$ accompanied by one additional water molecule $[SO_4^{2-},SO_2,2H^+,2H_2O]$.

The oxidative initiation reaction is not catalytic, but stoichiometric. Thus, the question arises, how long a catalyst may live, given that the concentration of sulfate on the surface of zirconia is finite. The current experiments show that the concentration of molecules to be oxidized, which are necessary to achieve an active catalyst, is surprisingly small. For a period of 10 h, only 0.88 μmol/g of sulfate/SO_3 was reduced. This corresponds to a ratio of approximately 500 butane molecules converted per SO_3 molecule reduced. A catalyst could, therefore, maintain its activity for 2000 h, assuming similar operating conditions. This "catalyst lifetime" was calculated by considering that approximately 40% of the total initial S content is associated with active/reducible active sites.[24] It is important to note that such small concentrations are formed continuously throughout the bed, avoiding high local concentrations and the danger of higher rates of the intermolecular reactions of condensation. This shows also why it is so difficult to add trace amounts of butenes to this and similar catalysts in order to achieve high and stable performance. The same chain length (500) was observed in the reaction of isobutane on SZ.[13] When the butane feed was "spiked" with butene, the reaction chain length decreased to 10−20.[25]

The important role of butene as initiating intermediate for *n*-butane isomerization on SZ was clearly demonstrated by the far higher catalytic activity in the presence of only 26 ppm butene (0.033 vs 0.018 μmol/g·s). Supporting indirect evidence for the present findings is provided by liquid phase catalysis. The oxidation of alkane during isomerization in a liquid acid also contributes to the initial step generating the active species. Ledford[26] proposed that the ionization of alkanes in superacid solutions proceeds by oxidation rather than by direct protonation because of the high oxidizing ability of SbF_5.[27] Moreover, the formation of SO_2[28] during *n*-butane isomerization in the presence of FSO_3H/HF acid and SbF_3 formation during activation of isobutane in SbF_5[29] are also such examples. The initial reaction of hexane in trifluoromethanesulfonic acid (TFMSA) under mild conditions was demonstrated to be dehydrogenation with the subsequent formation of alkenyl cations.[30]

The concentration of butenes in the reactant stream can be influenced by the presence of hydrogen and oxygen in the feed. Hydrogen could play a double role, that is, it could lower the concentration of butenes in the reactor[31] and/or it could stop the reactions of the carbenium ions by acting as a hydride transfer agent.[32] It has also been suggested by Garin et al.[21] that isobutene is rapidly hydrogenated on SZ at low temperature in the presence of hydrogen. In this context, it should be mentioned that the dissociation of molecular hydrogen on zirconia surface was reported to form surface Zr−H groups,[33] which could be very active for hydrogenation. While the present data do not suffice to distinguish between these two possibilities, the decrease of the catalytic activity with increasing of the hydrogen concentration in the feed suggests that the catalytic activity is directly related to the concentration of surface butene species.

It is noteworthy, on the other hand, that molecular oxygen acts as promoter for the initial step reaction. Given the low reaction temperature of 373 K, we think that this is achieved by oxygen creating/restituting a small concentration of oxidation sites (adsorbed SO_3 or pyrosulfates), which oxidize butane to butene. However, it should be mentioned that O_2^- species on the SZ surface have been observed by ESR spectroscopy after adsorption of *n*-butane[34] or benzene[35] and a subsequent treatment with dry O_2. For such a route, the formation of O_2^- species was attributed to the presence of Zr−H groups, which are formed on SZ with reacting *n*-butane. In the presence of oxygen, the negative effect of a high concentration of olefins was seen. As the rate of butene molecules formed exceeds the rate of hydride transfer in the carbenium ion chain reaction, alternate pathways for the reaction of butenes are preferred, such as oligomerization leading to rapid deactivation.

5. Conclusions

Butene species formed by oxidation of *n*-butane are shown to be the key intermediates during *n*-butane isomerization on SZ. Butene is formed by a reaction between butane and a labile

(24) Li, X.; Nagaoka, K.; Lercher, J. A. *J. Catal.* **2004**, *227*, 130−137.
(25) Tábora, J. E.; Davis, R. J. *J. Catal.* **1996**, *162*, 125−133.
(26) Ledford T. H. *J. Org. Chem.* **1979**, *44*, 23−25.
(27) Herlem, M. *Pure Appl. Chem.* **1977**, *49*, 107−113.
(28) Olah, G. A.; Farooq, O.; Husain, A.; Ding, N.; Trivedi, N. J.; Olah J. A. *Catal. Lett.* **1991**, *10*, 239−248.
(29) Culmann, J. C.; Sommer, J. *J. Am. Chem. Soc.* **1990**, *112*, 4057−4058.
(30) (a) Fărcaşiu, D.; Lukinskas, K. *J. Chem. Soc., Perkin Trans. 2* **1999**, *12*, 2715−2718. (b) Fărcaşiu, D.; Lukinskas, K. *J. Chem. Soc., Perkin Trans. 2* **1999**, *8*, 1609−1613. (c) Fărcaşiu, D.; Lukinskas, K. *J. Chem. Soc., Perkin Trans. 2* **2000**, *11*, 2295−2301.
(31) Weisz, P. B.; Swegler, E. W. *Science* **1957**, *126*, 31−32.
(32) Meusinger, J.; Corma, A. *J. Catal.* **1995**, *152*, 189−197.
(33) Kondo, J.; Sakata, Y.; Domen, K.; Maruya, K.; Onishi, T. *J. Chem. Soc., Faraday Trans.* **1990**, *86*, 397−401.
(34) Spielbauer, D.; Mekhemer, G. A. H., Bosch, E.; Knözinger, H. *Catal. Lett.* **1996**, *36*, 59−68.
(35) Chen, F. R.; Coudurier, G.; Joly, J. F.; Védrine, J. C. *J. Catal.* **1993**, *143*, 616−626.

SO_3/pyrosulfate-type surface species. For the first time, direct experimental evidence is given for all reaction products involved, and the thermodynamic feasibility of these reactions has been modeled by theoretical chemistry. The olefins formed induce a chain-type reaction that converts 500 butane molecules per butene formed. This allows SZ to reach acceptable lifetimes, and oxidative regeneration may lead to newly formed oxidation sites extending the lifetime further. Molecular hydrogen impedes the dehydrogenation reaction via pathways that are variants of hydride transfer. The presence of molecular oxygen induces reaction pathways to olefins, which rely on the generation of labile pyrosulfate/SO_3 entities on the surface and/or the generation of O_2^- anions. Whatever the mechanism of formation, the present study also shows that the reaction rate and the catalyst stability depend on the concentration of olefins and, in consequence, on the concentration of carbenium ions. At low concentration of butenes, the rate increases with the olefin concentration, and at high concentration, a high maximum activity is achieved, but the catalyst deactivates via formation of oligomers. The DFT calculations yield favorable reaction energies for the oxidative dehydrogenation of butane to butene by SZ, in particular, for sulfur loadings of two S atoms per (1 $\times$ 2) surface cell.

The evidence for the present pathway shows design strategies for new catalysts combining subtly anion-based redox chemistry with acid−base catalysis opening so new generic pathways for activating and functionalizing alkanes.

Acknowledgment. This work has been supported by the Deutsche Forschungsgemeinschaft (SPP 1091), the Fonds der Chemischen Industrie, and by a generous grant of computer time at the center for Bundeshöchstleistungsrechnen in Bayern. We also thank the Norddeutscher Verbund für Hoch- und Höchstleistungsrechnen for access to the IBM p690 turbo. Finally, we thank Prof. H. Papp and Prof. R. Schlögl as well as Dr. F. Jentoft, Dr. C. Breitkopf, Dr. S. Wrabetz, and Dr. K. Meinel for fruitful discussions.

JA054126D